

Broadband reflectance spectroscopy for establishing a quantitative metric of vascular leak using the Miles assay

John McMurdy

Brown University
Division of Engineering
Box D
Providence, Rhode Island 02912

Jonathan Reichner

Rhode Island Hospital
Department of Surgical Research
593 Eddy Street
Nursing Arts Building, Room 213
Providence, Rhode Island 02903

Zara Mathews

Brown University
Division of Biology & Medicine
Box G-A
Providence, Rhode Island 02912

Mary Markey

Hope High School
324 Hope Street
Providence, Rhode Island 02906

Sunny Intwala

Brown University
Division of Biology & Medicine
Box G-A
Providence, Rhode Island 02906

Gregory Crawford

University of Notre Dame
College of Science
168 Hurley Building
Notre Dame, Indiana 46556

1 Introduction

The vascular endothelium is not a simple, passive barrier to the passage of soluble and cellular blood components, but instead is subject to highly active and tightly regulated biological control. Under pathological conditions, barrier function may become compromised, leading to vascular leakage and concurrent tissue edema and inflammation. A number of inflammatory mediators affect the function of the vasculature, including vasoactive amines (e.g., histamine, serotonin), vasoactive peptides (e.g., substance P, CAP37), complement fragments (e.g., C3a, C4a, C5a), and lipid mediators (e.g., eicosanoids).¹⁻³ The mediators exert complex effects includ-

Abstract. Monitoring the physiological effects of biological mediators on vascular permeability is important for identifying potential targets for antivascular leak therapy. This therapy is relevant to treatments for pulmonary edema and other disorders. Current methods of quantifying vascular leak are *in vitro* and do not allow repeated measurement of the same animal. Using an *in vivo* diffuse reflectance optical method allows pharmacokinetic analysis of candidate antileak molecules. Here, vascular leak is assessed in mice and rats by using the Miles assay and introducing irritation both topically using mustard oil and intradermally using vascular endothelial growth factor (VEGF). The severity of the leak is assessed using broadband diffuse reflectance spectroscopy with a fiber reflectance probe. Postprocessing techniques are applied to extract an artificial quantitative metric of leak from reflectance spectra at vascular leak sites on the skin of the animal. This leak metric is calculated with respect to elapsed time from irritation in both mustard oil and VEGF treatments on mice and VEGF treatments on rats, showing a repeatable increase in leak metric with leak severity. Furthermore, effects of pressure on the leak metric are observed to have minimal effect on the reflectance spectra, while spatial positioning showed spatially nonuniform leak sites. © 2009 Society of Photo-Optical Instrumentation Engineers. [DOI: 10.1117/1.3233654]

Keywords: diffuse reflectance spectroscopy; edema; Miles assay; vascular leak; vascular endothelial growth factor.

Paper 09018R received Jan. 19, 2009; revised manuscript received Jul. 22, 2009; accepted for publication Jul. 24, 2009; published online Oct. 26, 2009.

ing vascular permeability, vasodilation, or vasoconstriction. Whereas increased vascular permeability may be a physiological accompaniment of normal host defense such as during wound healing, it can also be detrimental by providing easy access for tumor cell invasion of the bloodstream. The requirement of neovascularization for tumor progression has, in fact, led to several inhibitors of angiogenesis being evaluated as antitumor effectors.⁴

Diseases such as pulmonary edema, myocardial and cerebral infarction, diabetic retinopathy, and cancer metastasis all may benefit from the control and inhibition of vascular leak.^{5,6} In fact, vascular permeability factor (VPF) was originally identified as a tumor-associated protein capable of causing vascular leakage.⁷ This protein was later shown to be identical

Address all correspondence to: John McMurdy, Division of Engineering, Brown University, Box D, Providence, RI, 12912. Tel: 401-863-3078; Fax: 401-863-9120; E-mail: john_mcmurdy@brown.edu

to vascular endothelial growth factor (VEGF), so named because, in addition to its ability to cause vascular leak *in vivo*, it stimulated the growth of endothelial cells in culture.⁸ VEGF induces formation of small pores, or fenestrations, in the thin endothelial cell cytoplasm, which is responsible for the passive transport of solutes and small proteins.⁹ Leakage of larger proteins are due to junctional gaps between juxtaposed endothelial cells exposed to VEGF.⁶ Molecular mediators of endothelial permeability such as VEGF and other potential downstream signaling molecules are excellent targets for antivasular leak therapy.^{6,10} Alternatively, excess vasoconstriction is a significant aspect of the pathophysiology of diseases such as hypertension, renal failure, preeclampsia, and respiratory distress during episodes of asthma and emphysema.¹¹⁻¹⁴

The Miles assay is the most commonly employed *in vivo* indicator assay of vascular permeability.¹⁵ This assay detects extravasation of an intravenous injection of a dyed, radiolabeled, or fluoresceinated tracer protein such as albumin from the blood stream of a small animal to local sites in the skin where a permeability factor has been introduced intradermally. The lack of a method for quantifying vascular leak in an *in vivo* system, which in turn allows for repeated measurements on a single animal, restricts our basic understanding of the pathophysiology of vascular tone and hampers the pharmacokinetic analysis of lead molecules targeting endothelial function. This limitation is because the Miles assay is quantified primarily by observation, planimetry, or tissue extraction, although digital image analysis has more recently been studied.¹⁶ The former methods are inherently limited by imprecision or by restriction to a single measurement in time, and are particularly difficult in intradermal studies where tissue extraction is less precise.

The present study demonstrates the feasibility of broadband visible diffuse reflectance spectroscopy in conjunction with the Miles assay to establish a quantitative parameter correlated with vascular leak. Diffuse reflectance signals are collected using a visible spectral regime fiber optic reflectance probe coupled with broadband visible illumination to interrogate the degree of optical absorption in tissues of interest. Similar processes have been used in tissue analysis to characterize melanomas¹⁷ or quantify erythema¹⁸ and jaundice.¹⁹ This noninvasive procedure is reproducible and can be used to acquire repeated measures over time, allowing for pharmacokinetic analyses. Verification of this procedure was performed using both topical application of mustard oil and intradermal injection of recombinant VEGF into mice or rats to elicit vascular leak.

2 Methods

2.1 Rodent Preparation and Injection

Rats and mice were treated with both topical and injected irritants and controls over the course of this study. Fisher-344 rats (160 to 180 g; VAF-plus; Charles River Laboratories, Wilmington, Massachusetts) or BALB/c mice (~25 g; Charles River Laboratories) were housed in barrier cages and fed rat chow and water *ad libitum*. Rats and mice were both used to examine utility under differing skin properties, specifically the difference in tissue diffusion. Leak spots in mice tended to be more diffuse and nonuniform while leak spots in

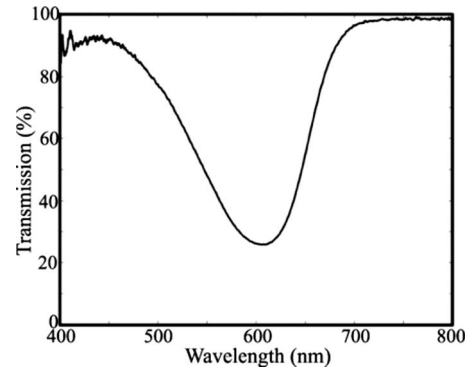


Fig. 1 Transmission spectra of Evans blue dye diluted to 0.1% with saline and with 1-cm path length. Note this solution is diluted from animal injected 2% solution due to longer cuvette path length.

rats tended to be more localized and uniform. VAF-plus rats and mice were certified free of common rat pathogens by the supplier and were monitored by Brown University/Rhode Island Hospital veterinary personnel. All animal studies followed current National Institutes of Health (NIH) guidelines for the use of laboratory animals and were performed according to Institutional Animal Care and Use Committee-approved protocols.

Vascular leak events are enhanced for measurement through the Miles assay, requiring preinjection of serum albumin conjugated with blue dye. Animals were anesthetized with 3% Isoflurane and shaved prior to intravenous injection with Evans blue dye-conjugated bovine serum albumin as a 2% saline solution.¹⁰ Optical absorption spectra of Evans blue dye is shown in Fig. 1. Dye-conjugated albumin was sterile filtered and warmed to 37° C prior to use. Rats were injected with 400 μ l and mice with 200 μ l of the dye-conjugated albumin solution based on protocols found to be successful in our laboratory. Edema was initiated immediately following injection using test agents. All mice/rats were shaved prior to data collection to eliminate hair absorption defects.

2.2 Signal Collection

The severity of leak was assessed qualitatively using digital photographs and postprocessing image analysis techniques, and assessed quantitatively using a fiber optic array diffuse reflectance probe. In the case of image analysis, digital photographs were taken under standard lighting at multiple time points following leak initiation. In addition to the raw image, "color normalized" images were constructed by calculating the ratio of blue channel intensity to red channel intensity at each pixel location, highlighting changes in relative channel intensity over uniform biasing of light intensity. False coloring is then applied to these images with boundaries around the minimum and maximum dye leak intensity to further highlight leak spots. Quantitative estimation based on these digital images was not performed, as this has been previously studied;¹⁶ rather, images are presented purely as supporting evidence showing leak sites and *relative* intensities of dye absorption at each site in each animal.

The fiber probe used for data collection is a commercially available construct—a metal ferrule with six 200- μ m glass fibers oriented in a hexagonal pattern around a single 200- μ m



Fig. 2 Photograph of data collection using a fiber probe at a vascular leak spot at the ear of a sedated mouse.

collection fiber manufactured by Ocean Optics (Dunedin, Florida). In this case, the ferrule was placed directly in contact with the animal and therefore no collimation optics were required. A high bandwidth white LED with emission spectra ranging from 430 to 730 nm was used for illumination along the six irradiation fibers, and collection fiber was affixed to a miniature static grating spectrometer with optical resolution of ~ 2 nm and operating range of 200 to 900 nm (USB4000, Ocean Optics, Dunedin, Florida). A photograph of data collection is shown in Fig. 2. Signal integration time ranged from 300 to 500 ms, dependent on skin pigment of the animal, with a white LED source broadband output optical power of 50 mW.

2.3 Data Processing and Leak Metric

Following injection of Evans blue and prior to introduction of a vascular leak promoter, a reflectance spectrum was collected from the physiological site of interest to remove baseline skin absorption characteristics. Spectra collected from leak-elicited sites were then postprocessed in multiple steps. First, skin spectra from leak spots were divided by baseline spectra to remove contributions from both skin background and LED emission. Next, skin spectra were normalized to the intensity at one spectral point ($\lambda_{\text{norm}}=725$ nm) to eliminate overall biasing of signals. This biasing is due to small fluctuations in probe orientation, causing shifts in the overall amount of light introduced to the tissue. The normalization point of 725 nm was selected as a point outside the strong dye absorption regions to scale spectra to a uniform level. Lastly, a linear fit was applied from two spectral points at the periphery of the Evans blue absorption spectra, specifically at $\lambda_1=450$ nm and $\lambda_2=725$ nm. This line was then subtracted from the spectra to eliminate any contributions to the spectral signatures attributed to oxy-/deoxyhemoglobin absorption and heterogeneity in the optical absorption. Removal of this fit line isolates the depth of the Evans blue absorption peak independently from any broad spectral variations in background absorption profiles from spot to spot on an individual animal. Following postprocessing, the absolute value of the intensity of Evans blue peak absorption at $\lambda_{\text{max}}=620$ nm is defined as the artificial quantitative leak metric and is given in arbitrary units where increasing values correspond to increasing leak intensity.

Specifically regarding the scattering effects in skin, increasing the amount of vascular leakage and subsequently edema has the effect of increasing the scattering coefficients in the skin. The subsequent decrease in penetration depth as a

result of increased scattering has the effect of decreasing absorption attributed to Evans blue dye, as well as distorting signals from frequency-dependent shift in scattering coefficients. The penetration depth variation with scattering coefficients has the effect of creating a system in which reflectance is nonlinear with dye concentration. The nonlinear relationship between reflectance and dye concentration is not studied in this disclosure, but will be explored in further studies in conjunction with tissue extraction correlating *in vitro* dye leak concentration estimation with *in vivo* measurements. With respect to signal distortion, the linear fit at the periphery of albumin dye absorption rejects much of the distortion and allows leak metric to focus primarily on signal variation attributed to dye.

3 Results

Control experiments and three sets of evaluation experiments were conducted to validate the operation of the probe, two on mice and one on rats. Identical data collection techniques were applied in all studies.

3.1 Controls for Pressure and Spatial Leak Variability

Two relevant parameters to consider regarding the reliability and repeatability of fiber probe data collection are the effects of spatial variability at the vascular leak site, and variability in reflectance spectra with changing pressure of the probe on the skin. Both factors were examined prior to additional investigation.

Vascular leak was introduced to a dye-injected mouse using a topical application of 1% mustard oil on the torso along with topical application of acetone as a vehicle control. Mustard oil, a chemical irritant, is a potent inducer of neurogenic inflammation and vascular permeability when applied topically, although the mechanism by which it causes vascular leak has not been fully elucidated.²⁰ Pressure variation was quantified by collecting multiple spectra in succession starting with the probe gently resting on the leak spot with an approximate force of 100 mN and subsequently increasing the pressure to approximately 1 N using masses clamped to the optical probe. This was performed on three different spatial locations of the mustard oil treatment site (two at the central location, one at the periphery) and one location on the acetone treatment site. As shown in Fig. 3(a), the intensity of the leak spot and leak metric is highly uniform with pressure for all three mustard oil treatment sites with standard deviation (SD) $<3\%$ of mean leak metric in all three sites, and SD of all three sites within 1% of the maximum leak metric in the respective site. As this result shows, this data collection method likely does not require additional controls for pressure variability between probe and tissue.

Spatial probe positioning was observed to add more variability in the quantification of leak than pressure variation. An order of magnitude assessment of spatial variation in a vascular leak spot was obtained using the same mustard oil treatment and scanning multiple points in succession along one dimension across the spot. A plot of the leak metric versus arbitrary spatial position while physically translating across a mustard oil leak site is shown in Fig. 3(b). Spatial variability in dye peak depth and subsequent leak metric is of significance; in this case, the SD is 7% across the center of the

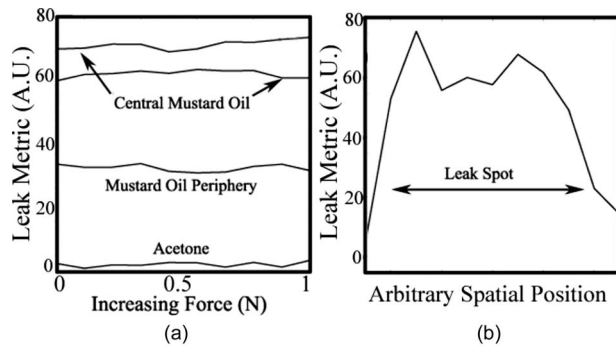


Fig. 3 (a) Plot of the quantitative leak metric as a function of the approximate force of probe pressed against skin on an acetone treatment site, the periphery of a mustard oil treatment site, and the two positions at the center of a mustard oil treatment site. (b) Plot of the leak metric as a function of arbitrary spatial position as the probe is physically translated across the spot showing the spatial heterogeneity of vascular leak.

mustard oil treatment site and increasing significantly at the periphery. This may be a result of dye diffusion in subcutaneous and cutaneous tissue layers, blood vessel positioning, injection variability, or any number of other effects. The analytical result of this fluctuation will be noise introduction to curves tracking the vascular leak metric as a function of time. Spatial fluctuations can be removed by either fixing the probe over the leak spot to reduce spatial variation with each time sampling point, or applying an averaging filter to create a function representative of the average time course leak across the spot. The latter method is employed here, as a scanning average filter is applied to the time course functions generated in the following experiments to smooth the noise generated through spatial variability, and to obtain a more accurate representation of physiological phenomena.

3.2 Topical Mustard Oil and Acetone in Mice

Vascular leak was initiated by topical application of 1% mustard oil to one ear and one spot on the body of a mouse. An acetone control was applied in the contralateral ear and a separate spot on the body. Background spectra were collected prior to topical application but following introduction of dye to blood stream, and spectra were collected at 5-min intervals for 60 min. A plot of the postprocessed spectra at 0 and 60 min are shown in Figs. 4(a) and 4(b), respectively. Note that as a result of the postprocessing applied to the signals, the intensity of each reflectance spectra is in arbitrary units (not absorption units or percent transmission), where decreasing intensity corresponds to decreased reflected intensity. These spectra show the anticipated increase in Evans blue absorption from 0 to 60 min for both the ear and body treatment compared with spectra from acetone. Additionally, in both the mustard oil and acetone ear treatments at times 0 and 60 min, absorption signatures from hemoglobin (double peak around 550 nm) are observed as a result of the proximity of blood vessels to the skin surface. However, background subtraction and postprocess fitting remove most of the contamination of pure albumin dye signals, and the spectral absorption of hemoglobin does not significantly overlap the Evans blue dye peak absorption at 620 nm.

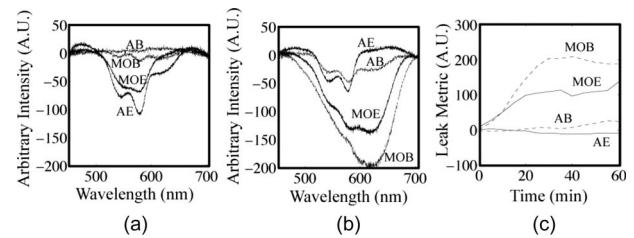


Fig. 4 Normalized diffuse reflectance spectra of mustard oil (MO) and acetone (A) treatment sites at the ear (MOE/AE) and on the body (MOB/AB) of a mouse at (a) time = 0 min, and (b) after 60-min elapsed time. (c) Leak metric as a function of time for mustard oil and saline on the ear and skin. Note the appearance of hemoglobin absorption spectra in ear measurements as blood vessels are proximal to surface and tissue is highly transparent.

The time progression of the mustard oil leak is plotted in Fig. 4(c), showing the expected increase in leak metric for mustard oil in the ear and body compared to acetone. As anticipated, more leak is observed in the body as a result of a higher vascular density responding to the irritation stimulus. The results of this experiment were representative of two additional mice examined with this same mustard oil and acetone topical treatment. A raw digital image of the mouse analyzed in Fig. 4 is shown in Fig. 5(a), and a color normalized image is shown in Fig. 5(b), calculated as discussed in Sec. 2.2.

3.3 Subcutaneous Vascular Endothelial Growth Factor and Saline in Mice

Subdermal injections were subsequently examined using the same probe configuration. Mouse vascular endothelial growth factor (mVEGF, BioSource, Camarillo, California) was used as the agent in this study. Explicitly, vascular endothelial growth factor was investigated as a well-known mediator of vascular leak, and saline was used as a control to observe leak effects of the injection itself. Subcutaneous injections of 100 μ L of VEGF at 10 mg/mL and 100 μ L of saline were introduced in three separate animals. Postprocessing steps were applied to data and the leak metric plotted versus time for at least 40 min in 5-min intervals for three mice, denoted mice 1, 2, and 3 and shown in Figs. 6(a)–6(c).

The increase in dye absorption at the VEGF treatment site was observed as the maximum effect in all three mice, while saline was observed to have comparatively less absorption effects. In all three animals, the time course progression of the leak is roughly that of an inverse exponential, showing that the majority of leak occurs at the early stages of injection and

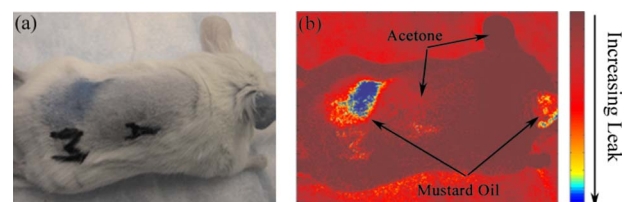


Fig. 5 (a) Raw digital image of topical mustard oil and acetone irritations on the body and ear and (b) the color normalized version of the image calculated as described in Sec. 2.2. (Color online only.)

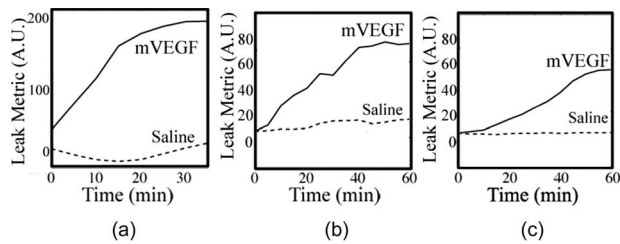


Fig. 6 Leak metric as a function of time for subcutaneous injections of VEGF and saline in (a) mouse 1, (b) mouse 2, and (c) mouse 3. Note that a negative leak metric results from small difference in skin absorption properties relative to background normal skin spectra, translating to a negative value when the two are ratioed and creating this artifact.

continues for as much as 50 min after the initial irritation. The maximum leak metric showed high variability in its maximum value ($SD \approx 60\%$ of mean leak metric in this small set), particularly in the case of mouse 1 with respect to the other two mice, indicating that the quantitative amount of leak can vary significantly from subject to subject with uniform treatments. This variability in the amount of VEGF leak between three mice can be a result of numerous factors, including the depth of injection, age, and weight of an animal, and localization of vasculature. However, the focus here is on the ability to quantify the leak, not to ascertain the underlying mechanisms of intrasubject leak variability.

Color normalized images of mice 1 and 2 at the time point of maximum leak metric are shown in Figs. 7(a) and 7(b), respectively. This image again shows an approximation, using false color, of the intradermal injection sites and an estimate of leak intensity (the third spot is an undisclosed investigational protein also injected intradermally). It is emphasized that these images are rough quantitative measures of leak; however, these images show what is expected: a significantly increased leak intensity for mouse 1 versus mouse 2, as observed in spectral analysis shown in Fig. 6.

3.4 Subcutaneous Vascular Endothelial Growth Factor and Saline in Rats

It was found that the greater thickness of rat skin as compared to mice permits intradermal injections that produce a more spatially homogeneous dye spot; therefore, rats were investigated in a similar experiment to the mouse VEGF/saline experiment. Of two rats included in data analysis, one received subcutaneous injections of 100 μ L of mouse VEGF at 10 mg/mL and saline. The second rat received subcutaneous

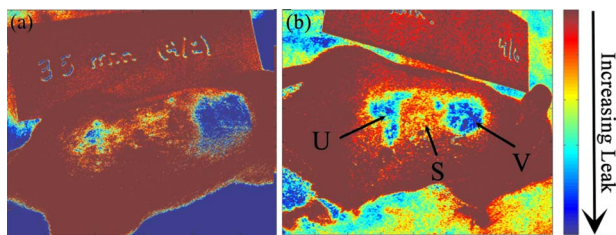


Fig. 7 Color normalized images of two of the mouse subjects, (a) mouse 1 and (b) mouse 2 showing leak spots of VEGF (V), saline (S), and a third undisclosed protein (U). (Color online only.)

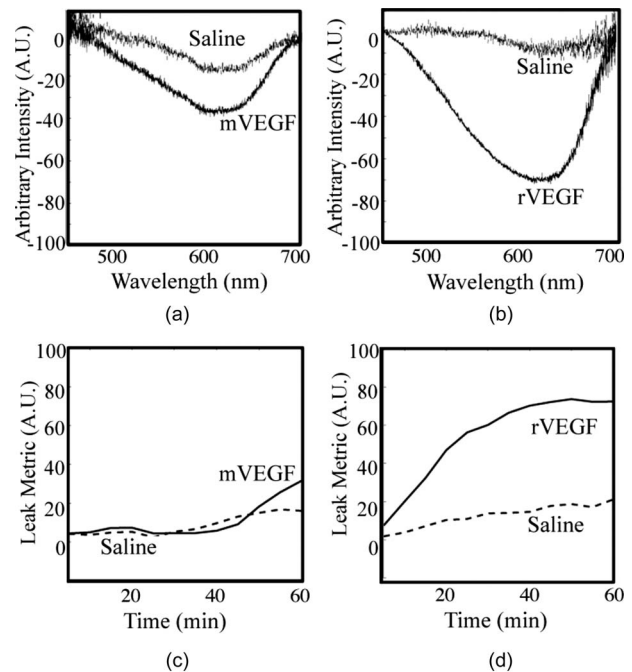


Fig. 8 Plot of reflection spectra at $T=60$ min for two rat subjects, (a) rat 1 with injections of mouse VEGF and saline, and (b) rat 2 with injections of rat VEGF and saline. Plot of the leak metric as a function of time for (c) rat 1 and (d) rat 2.

ous injections of 100 μ L of rat VEGF (BioSource, Camarillo, California) at 10 mg/ml and saline. The two different VEGF species were used to investigate intentional differences in leak promotion efficiency. Data were again collected at 5-min increments for 60 min in each animal with postprocessing applied. The processed reflection spectra at a time of 60 min for rats 1 and 2 are shown in Figs. 8(a) and 8(b), respectively, while the resulting leak metric is plotted as a function of time for both rats in Figs. 8(c) and 8(d), respectively. The leak metric versus time plots show that in the same dosage, recombinant rat VEGF is shown to induce significantly more leak, approximately four times greater than the mouse VEGF. Saline in both cases again had a negligible effect in these animals. In the case of the mouse VEGF, the leak induced in a rat by the VEGF intended for another species had leak of minimal significance above that of the saline spot.

Color-corrected images were more difficult to construct in rats because of the stronger skin pigment distorting the color channels, such that the spots are not clearly visible, and as such, the data are not pictured here.

4 Discussion

The target goal of this study was to identify the suitability of a noninvasive method in quantifying vascular leak. These proof of principle results validate the ability to create a vascular leak metric correlated with leak intensity. This technique has the advantage that it may be performed in real time to assess not only the intensity of leak, but also the kinetics of permeability change, highlighting the most significant effects of potential leak promoters and inhibitors in pharmacological

analysis. This technique can be performed with standard spectrophotometry equipment and relatively standard fiber optic sampling probes.

It was noted that spatial variability in leak due to diffusion of dye has an effect and needs to be controlled through data collection or noise reduction. This spatial variability is likely dependent on the diffusivity of albumin molecules in the tissue sampled, and can potentially be corrected by collection of spectra over a wider area of the leak-induced spot. The spectra can then be averaged over this wide area to better represent the quantitative degree of leak without spatial variation. While a filter was applied to the data presented here to remove some effects of spatial leak variation, a more ideal method to study the spatial properties of vascular leak would be hyperspectral imaging, which pixel by pixel resolves the intensity of albumin dye independent of skin and blood absorbers. It was also verified that the pressure of the probe on the sample has little effect on the signal, making data collection more robust.

Data shown in this disclosure indicate a repeatable increase in vascular leak metric with increasing leak intensity, and can be used to quantitatively differentiate the effectiveness of various biomolecules in changing endothelial permeability. Future studies to validate this technique require comparison of this method of leak measurement with accepted methods of tissue extraction and subsequent dye extraction from excised tissue. This is most straightforwardly performed in ear measurements, as excision is straightforward and dye can easily be removed from tissue. Additionally, a larger sample set of mice, rats, and other species need to be enrolled to further strengthen the significance of this technique for biological researchers studying immune response related to endothelial barrier function.

Changes in vascular permeability may be disease related or a consequence of new vessel growth. *In vivo* screening for effects of therapeutics or toxins is integral in ruling out undesired side effects or in developing new compounds designed expressly for inhibition of edema or neovessel in growth. Work shown in this report offers a new approach to assessing vascular leak *in vivo*, and contains the inherent advantage of repeated measures, thereby maximizing the information that may be obtained from each experimental animal. This technique can be an easily implemented method in future immunology studies.

Acknowledgments

Funding is acknowledged from the NASA GSRP Fellowship Program (NNG05GL57H) and the RI Science and Technology Advisory Council (STAC) grant. No conflicts of interest exist for all authors of this paper

References

1. N. Gautam, A. M. Olofsson, H. Herwald, L. F. Iversen, E. Lundgren-Akerlund, P. Hedqvist, K. E. Arfors, H. Flodgaard, and L. Lindbom, "Heparin-binding protein (HBP/CAP37): a missing link in neutrophil-evoked alteration of vascular permeability," *Nat. Med.* **7**, 1123–1127 (2001).
2. K. Ley, C. Laudanna, M. I. Cybulsky, and S. Nourshargh, "Getting to the site of inflammation: the leukocyte adhesion cascade updated," *Nat. Rev. Immun.* **7**, 678–689 (2007).
3. R. Medzhitová, "Origin and physiological roles of inflammation," *Nature (London)* **454**, 428–435 (2008).
4. O. Benny, O. Fainaru, A. Adini, F. Cassiola, L. Bazinet, I. Adini, E. Pravda, Y. Nahmias, S. Koirala, G. Corfas, R. J. D'Amato, and J. Folkman, "An orally delivered small-molecule formulation with antiangiogenic and anticancer activity," *Nat. Biotechnol.* **26**, 799–807 (2008).
5. G. P. VanNieuwAmerongen, C. M. L. Beckers, I. D. Achekar, S. Zeeman, R. J. P. Musters, and V. W. M. v. Hinsbergh, "Involvement of rho kinase in endothelial barrier maintenance," *Arterioscler., Thromb., Vasc. Biol.* **27**, 2332–2339 (2007).
6. S. M. Weis and D. A. Cheresh, "Pathophysiological consequences of VEGF-induced vascular permeability," *Nature (London)* **2005**, 497–505 (2005).
7. D. R. Senger, S. J. Galli, A. M. Dvorak, C. A. Perruzzi, V. S. Harvey, and H. F. Dvorak, "Tumor cells secrete a vascular permeability factor that promotes accumulation of ascites fluid," *Science* **219**, 983–985 (1983).
8. P. J. Keck, S. D. Hauser, G. Krivi, K. Sanzo, T. Warren, J. Feder, and D. T. Connolly, "Vascular permeability factor, an endothelial cell mitogen related to PDGF," *Science* **246**, 1309–1312 (1989).
9. W. G. Roberts and G. E. Palade, "Increased microvascular permeability and endothelial fenestration induced by vascular endothelial growth factor," *J. Cell. Sci.* **108**, 2369–2379 (1995).
10. J. Doukas, W. Wrasidlo, G. Noronha, E. Dneprovskaiia, R. Fine, S. Weis, A. Hood, A. DeMaria, R. Soll, and D. A. Cheresh, "Phosphoinositide 3-kinase γ/δ inhibition limits infarct size after myocardial ischemia/reperfusion injury," *Proc. Natl. Acad. Sci. U.S.A.* **103**, 19866–19871 (2006).
11. J. S. Gilbert, M. J. Ryan, B. B. LaMarca, M. Sedeek, S. R. Murphy, and J. P. Granger, "Pathophysiology of hypertension during preeclampsia: linking placental ischemia with endothelial dysfunction," *Clin. Neurophysiol.* **294**, H541–H550 (2008).
12. S. Polikepahad, R. M. Moore, and C. S. Venugopal, "Endothelins and airways—a short review," *Res. Commun. Mol. Pathol. Pharmacol.* **119**, 3–51 (2006).
13. T. Watson, P. K. Goon, and G. Y. Lip, "Endothelial progenitor cells, endothelial dysfunction, inflammation, and oxidative stress in hypertension," *Antiox. Redox Signal.* **10**, 1079–1088 (2008).
14. J. R. Wu-Wong, "Endothelial dysfunction and chronic kidney disease: treatment options," *Curr. Opin. Invest. Drugs* **9**, 970–982 (2008).
15. A. A. Miles and E. M. Miles, "Vascular reactions to histamine, histamine liberator and leukotaxin in the skin of guinea pigs," *J. Physiol. (London)* **118**, 228–257 (1952).
16. N. McClure, D. M. Robertson, P. Heyward, and D. L. Healy, "Image analysis quantification of the Miles assay," *J. Pharmacol. Toxicol. Methods* **32**, 49–52 (1994).
17. G. Zonios, A. Dimou, I. Bassukas, D. Galaris, A. Tsolakidis, and E. Kaxiras, "Melanin absorption spectroscopy: new method for noninvasive skin investigation and melanoma detection," *J. Biomed. Opt.* **13**, 014017 (2008).
18. G. N. Stamatias, B. Z. Zmudzka, N. Kollias, and J. Z. Beer, "In vivo measurement of skin erythema and pigmentation: new means of implementation of diffuse reflectance spectroscopy with a commercial instrument," *Br. J. Dermatol.* **159**, 683–690 (2008).
19. L. L. Randeberg, E. B. Roll, L. T. N. Nilsen, T. Christensen, and L. O. Svaasand, "In vivo spectroscopy of jaundiced newborn skin reveals more than a bilirubin index," *Acta Paediatr.* **94**, 65–71 (2005).
20. A. N. Akopian, N. B. Ruparel, A. Patwardhan, and K. M. Hargreaves, "Cannabinoids desensitize capsaicin and mustard oil responses in sensory neurons via TRPA1 activation," *J. Neurosci.* **28**, 1064–1075 (2008).